

TR-88-25

DTIC FILE COPY

AD-A193 243

The Role of Lithium Passivation in LiSO_2

Prepared by

H. F. BITTNER

Chemistry and Physics Laboratory
Laboratory Operations
The Aerospace Corporation
El Segundo, CA 90245

29 December 1986

Prepared for

SPACE DIVISION
AIR FORCE SYSTEMS COMMAND
Los Angeles Air Force Station
P.O. Box 92960, Worldway Postal Center
Los Angeles, CA 90009-2960

APPROVED FOR PUBLIC RELEASE:
DISTRIBUTION UNLIMITED

DTIC
ELECTE
MAR 10 1988
S H D

3 8 3 5 0 8 3

This report was submitted by The Aerospace Corporation, El Segundo, CA 90245, under Contract No. F04701-85-C-0086 with the Space Division, P.O. Box 92960, Worldway Postal Center, Los Angeles, CA 90009. It was reviewed and approved for The Aerospace Corporation by S. Feuerstein.

Capt Thomas Wetterstroem was the project officer for the Mission-Oriented Investigation and Experimentation (MOIE) Program.

This report has been reviewed by the Public Affairs Office (PAS) and is releasable to the National Technical Information Service (NTIS). At NTIS, it will be available to the general public, including foreign nationals.

This technical report has been reviewed and is approved for publication. Publication of this report does not constitute Air Force approval of the report's findings or conclusions. It is published only for the exchange and stimulation of ideas.

Thomas Wetterstroem

THOMAS WETTERSTROEM, Capt, USAF
MOIE Project Officer
SD/CWASB

Raymond M. Leong

RAYMOND M. LEONG, Major, USAF
Deputy Director, AFSTC West Coast Office
AFSTC/WCO OL-AB

UNCLASSIFIED

SECURITY CLASSIFICATION OF THIS PAGE

A193 243

REPORT DOCUMENTATION PAGE

1a. REPORT SECURITY CLASSIFICATION Unclassified			1b. RESTRICTIVE MARKINGS		
2a. SECURITY CLASSIFICATION AUTHORITY			3. DISTRIBUTION/AVAILABILITY OF REPORT Approved for public release; distribution unlimited.		
2b. DECLASSIFICATION/DOWNGRADING SCHEDULE					
4. PERFORMING ORGANIZATION REPORT NUMBER(S) TR-0086(6945-01)-1			5. MONITORING ORGANIZATION REPORT NUMBER(S) SD TR 88-25		
6a. NAME OF PERFORMING ORGANIZATION The Aerospace Corporation Laboratory Operations		6b. OFFICE SYMBOL (If applicable)	7a. NAME OF MONITORING ORGANIZATION Space Division		
6c. ADDRESS (City, State and ZIP Code) El Segundo, CA 90245			7b. ADDRESS (City, State and ZIP Code) Los Angeles Air Force Station Los Angeles, CA 90009-2960		
8a. NAME OF FUNDING/SPONSORING ORGANIZATION Space Division		8b. OFFICE SYMBOL (If applicable)	9. PROCUREMENT INSTRUMENT IDENTIFICATION NUMBER F04701-85-C-0086-P00016		
8c. ADDRESS (City, State and ZIP Code) Los Angeles, CA 90009-2960			10. SOURCE OF FUNDING NOS.		
			PROGRAM ELEMENT NO.	PROJECT NO.	TASK NO.
			WORK UNIT NO.		
11. TITLE (Include Security Classification) The Role of Lithium Passivation in LiSO_2					
12. PERSONAL AUTHOR(S) Harlan F. Bittner					
13a. TYPE OF REPORT		13b. TIME COVERED FROM _____ TO _____		14. DATE OF REPORT (Yr., Mo., Day) 29 December 1986	
				15. PAGE COUNT 25	
16. SUPPLEMENTARY NOTATION					
17. COSATI CODES			18. SUBJECT TERMS (Continue on reverse if necessary and identify by block number)		
FIELD	GROUP	SUB. GR.	Li/SO ₂ Batteries, Passivation, Self-discharge, Storage, Performance ←		
19. ABSTRACT (Continue on reverse if necessary and identify by block number) The role of the lithium passivation layer on lithium sulfur dioxide (Li/SO_2) cell performance has been studied. Polarization attributed to the Li layer was characterized; an initial polarization (voltage delay) was in some cases followed by a secondary polarization. It was found that long-term, low rate discharge modified the Li passivation layer, which resulted in increased Li corrosion and decreased cell capacity. The degradation was greater at high temperature. Short-term partial discharge was also found to result in increased Li corrosion. Analysis of formation of the Li layer was studied by surface analytical techniques. Results were interpreted in terms of a primary layer, which was responsible for the passivation, and a thicker, porous secondary layer. Formation of the secondary layer is exacerbated by partial discharge. The secondary layer results from precipitation of the Li corrosion products, and was identified to contain $\text{Li}_2\text{S}_2\text{O}_5$, $\text{Li}_2\text{S}_2\text{O}_6$, and $\text{Li}_2\text{S}_n\text{O}_6$, where $n > 2$. The primary layer is responsible for the initial polarization (voltage delay) under load whereas the secondary layer induces a second polarization that inhibits high-rate discharge.					
20. DISTRIBUTION/AVAILABILITY OF ABSTRACT UNCLASSIFIED/UNLIMITED <input checked="" type="checkbox"/> SAME AS RPT. <input type="checkbox"/> DTIC USERS <input type="checkbox"/>			21. ABSTRACT SECURITY CLASSIFICATION Unclassified		
22a. NAME OF RESPONSIBLE INDIVIDUAL			22b. TELEPHONE NUMBER (Include Area Code)		22c. OFFICE SYMBOL

CONTENTS

I. INTRODUCTION.....	3
II. BACKGROUND.....	5
III. EXPERIMENTAL.....	9
IV. RESULTS AND DISCUSSION.....	9
1. Passivation-Layer-Induced Polarization.....	9
2. Effect of Low Discharge Rates.....	11
3. Chemistry of the Lithium Passivation Layer.....	14
4. Kinetics of Passivation Layer Growth.....	17
V. CONCLUSIONS.....	23
REFERENCES.....	25



Accession For	
NTIS CR&I	<input checked="" type="checkbox"/>
DTIC TAB	<input type="checkbox"/>
Unannounced	<input type="checkbox"/>
Justification	
By	
Distribution/	
Availability Codes	
Avail and/or	
Dist Special	
A-1	

FIGURES

1.	Polarization of previously-undischarged and previously-partially discharged Li electrode (vs Li reference) in SO_2 electrolyte solution under 12.5 mA/cm^2 discharge.....	10
2.	Time dependence of Li/SO_2 capacity delivered at 70°F under continuous 500 microamp discharge with weekly pulses.....	12
3.	Temperature dependence of Li/SO_2 capacity delivered after 26 weeks of continuous 500 microamp discharge with weekly pulses.....	13
4.	IMMA results for (A) undischarged and (B) partially discharged Li electrodes from Li/SO_2 cells.....	15
5.	FTIR spectra of the Li passivation layer for undischarged and partially discharged Li electrodes from Li/SO_2 cells.....	16
6.	Impedance of Li electrode stored open circuit in SO_2 electrolyte.....	18
7.	Primary Li layer thickness as function of $t^{1/2}$	19
8.	Reciprocal of capacitance versus resistance for primary layer on undischarged Li electrode in SO_2 electrolyte.....	10
9.	Effect of partial discharge on Li primary layer and Li corrosion.....	22

I. INTRODUCTION

The lithium sulfur dioxide (Li/SO_2) electrochemical couple has been widely used by the military for low- to moderate-rate applications, and has recently found application in missile use for high-rate application. Li/SO_2 batteries are attractive because they have high energy density, excellent low temperature performance, and long storage life. The long storage life is a direct consequence of the lithium passivation layer, which inhibits lithium corrosion by the electrolyte solution. On the other hand, the lithium passivation layer induces a polarization upon loading the cell. In some cases the induced polarization severely affects performance.

We have studied several aspects of lithium passivation in the Li/SO_2 couple in our laboratory. These include the polarization effects of both a primary and a secondary Li passivation layer; impact of low discharge rates on the Li passivation and cell storage life; and the chemistry and kinetics of the growth of the primary and secondary Li passivation layers.

II. BACKGROUND

Limited work has been performed to study the Li/SO_2 performance characteristics that are impacted by the Li passivation layer. Storage life studies, polarization due to the primary passivation layer (voltage delay), and some chemical characterization of the passivation layer have been investigated.

Voltage delay characteristics in Li/SO_2 cells were tabulated by Bro (1). Discharge at low temperatures following high temperature storage exacerbates the delay. High temperature storage increases the rate of the lithium passivation layer formation and the low temperatures limit diffusion processes, thereby increasing the polarization of the passivation layer. Bro (1) reported negligible voltage delays at room temperature and delays as long as 90 seconds at -30°C at 3 Amps on a "D" cell.

Li/SO_2 cells are purported to have a 10-year shelf life. Five-year shelf life with less than 5 - 10% capacity loss has been demonstrated (2). Capacity losses at 71°C of less than 1.5% per month have been reported (2). Much of this degradation can be attributed to lithium corrosion.

Low discharge rates during storage have been reported to result in higher degradation rates, presumably through increased lithium corrosion rate. Levy (3) reported more than 50% capacity loss after one year for cells that were discharged at 100 microamps with pulses (8 mA for 150 msec every 15 sec) over a temperature cycle from -40 to 71°C . Constant discharge without the pulsing resulted in between 4 and 10% capacity loss after 6 months. Bro (1) points out that lithium corrosion can also result in increased anode polarization, in addition to anode consumption; the increased polarization may reduce available high-rate capacity, whereas the consumption reduces capacity at all rates.

Limited work has been performed to study the chemical composition of passivation layers on the lithium electrode in Li/SO_2 cells. It has often been assumed and generally accepted (4) that the passivation layer is comprised of lithium dithionite ($\text{Li}_2\text{S}_2\text{O}_4$), the discharge reaction product in

the Li/SO₂ cell. Conversely, Kilroy and Anderson (5) found Li₂SO₄, Li₂SO₃, and Li₂S and no dithionite on the lithium, as studied by mass spectrometry and scanning Auger spectroscopy. Abraham and Chaudhri (6) used IR and XPS techniques to study lithium films from aged and partially discharged Li/SO₂ cells. They reported finding Li₂S, Li₂S₂O₄, Li₂SO₃, Li₂S_nO₆ (n>2), and Li₂S₂O₅.

Although considerable work has been performed to study the kinetics of lithium film growth in Li/SOCl₂ cells, little work has been performed on the Li/SO₂ couple. Gerenov et al. (7, 8) studied passive films on lithium in Li/SO₂ cells by galvanostatic pulse techniques and AC impedance. They found a parabolic growth rate and a specific conductivity of about 10⁻⁹ (ohm-cm)⁻¹ for the Li passivation layer.

Peled (9) developed a model to describe the film formation in the Li/SOCl₂ couple in terms of a solid electrolyte interphase (SEI); his model has application to the Li/SO₂ couple as well. According to the SEI model, a perfect single crystal passivation layer acts as a solid electrolyte that conducts lithium ions but is an electronic insulator. In a real, multicrystalline passivation layer, however, growth occurs by electronic conduction via grain boundaries or cathodic impurities in the layer. The passivation layer growth is parabolic

$$L = (2KV_e t/Z)^{1/2} \quad (1)$$

where L is the layer thickness, K the rate constant, V_e the potential drop across the layer, t the time, and Z is the specific electronic impedance. Actual growth rates would likely deviate from parabolic rates, possibly due to changes in Z with L, such as induced by cracks or defects in the layer.

III. EXPERIMENTAL

Experimental results described below were obtained on either commercial Li/SO₂ cells or laboratory Li/SO₂ cells. Commercial cells used were either "D" or "DD" size with a spiral wound configuration. Laboratory cells were constructed of heavy-walled Pyrex cell cases to contain the pressurized electrolyte solution. Lithium working, counter, and reference electrodes were used. The electrolyte solution contained 0.5M LiBr in acetonitrile/SO₂. Materials were dried prior to assembling the cells in an Argon-filled dry box.

The laboratory cells were used to study the effects of partial discharge. Open circuit impedance measurements were taken immediately after cells were filled with the electrolyte solution; the impedance technique has been described earlier (10,11). Some cells were allowed to stand open circuit up to several months, while other cells were given intermittent discharges (5 min. at 12.5 mA/cm²). Recovery of the open circuit impedance was monitored immediately upon terminating the discharge.

Commercial cells were also used to study the effects of partial discharge. In these cases, cells were given partial discharges at approximately 14 mA/cm², removing up to 20% of their capacity. Other commercial cells were tested over a six-month period for capacity retention under continuous low discharge rates. Cells were discharged with a continuous 500 microamp load with weekly 10-minute 600 mA pulses. Cells were discharged at 70°F, 105°F, and 120°F for up to 27 weeks. At the end of the test period, cells were discharged at 70°F at 600 mA to 2.0 V/cell. The complete test matrix is given in the reference (12).

Lithium surfaces from both commercial and laboratory cells were studied by Ion Microprobe Mass Analysis (IMMA), Fourier Transform Infrared Spectroscopy (FTIR), and X-ray Photoelectron Spectroscopy (XPS).

IV. RESULTS AND DISCUSSION

1. Passivation-Layer-Induced Polarization

The Li passivation layer induces a polarization or voltage drop under load. The polarization that occurs immediately after applying a load is often referred to as the voltage delay. We have described a second polarization phenomenon which we have attributed to a secondary passivation layer (10,11). These polarization phenomena are depicted in Figure 1, in which the load voltages of undischarged and partially-discharged Li electrodes are given. The cell that had been stored 4 weeks undischarged exhibited an initial voltage drop (voltage delay), which was caused by a thin primary passivation layer. The cell that had been partially discharged over the 4-week period showed the expected primary polarization, but then exhibited a secondary polarization, caused by a secondary passivation layer. Formation of the primary and secondary passivation layers will be discussed below.

Both the primary and secondary polarization phenomena are caused by charge carrier polarization under load. Although the SEI is a lithium ion conductor, the conductivity is insufficient to support a normal discharge. As the lithium ions are depleted during discharge in the electrolyte solution, the cell voltage drops and a lithium ion gradient is established within the passivation layer during discharge.

The voltage recovers with continued discharge as the lithium passivation layer is modified, reducing the polarization. The mechanism by which the passivation layer is modified is not well understood; the layer may simply crack from thermal stresses induced by the polarization or as supporting lithium is consumed. It is likely that under discharge, even at high rates, a modified passivation layer persists; lithium reacts exothermally with the electrolyte solution, and in the absence of any passivation layer, a runaway reaction could be expected.

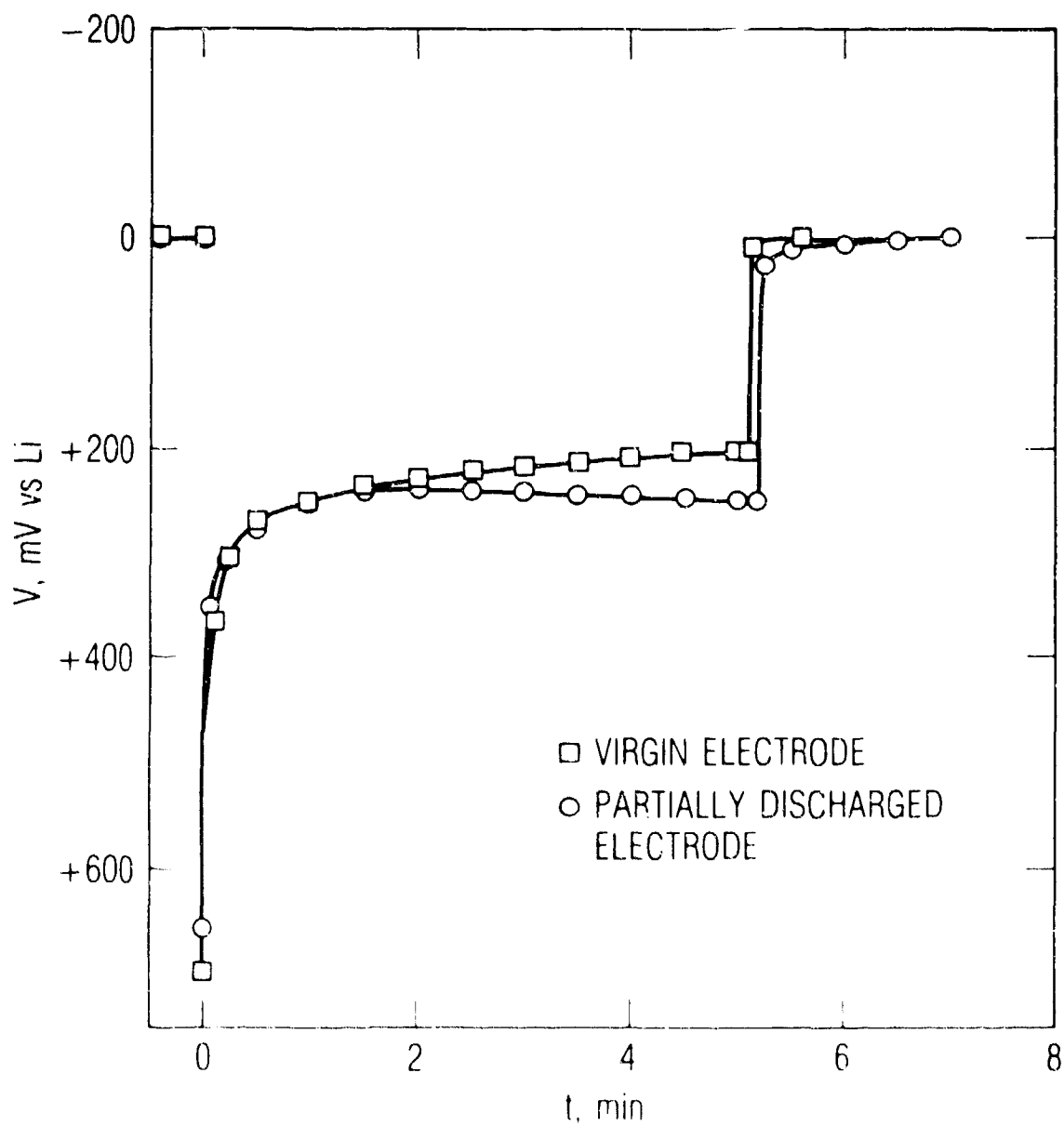


Fig. 1 Polarization of previously-undischarged and previously-partially-discharged Li electrode (vs Li reference) in SO_2 electrolyte solution under 12.5 mA/cm^2 discharge. Region A indicates the primary polarization (voltage delay) and region B indicates the secondary polarization effect.

2. Effect of Low Discharge Rates

As part of an effort to determine the effects of continuous low discharge rates on cell storage life, commercial Li/SO₂ cells were stored under low discharge conditions up to six months at different temperatures.

The dependence of delivered cell capacity on discharge time for the 70°F results is given in Figure 2. A significant reduction in delivered capacity is evident after 18 weeks of discharge, although no capacity loss is apparent up to 18 weeks. The temperature dependence of the total capacity after 27 weeks discharge is given in Figure 3. The capacity reduction is greater at higher temperatures; a capacity loss of as much as 20% is apparent after 27 weeks at 120°F.

Post mortem of several cells indicated that the lithium was almost completely consumed. This implies that the capacity loss occurred because of lithium corrosion.

The cells that were discharged after 9 and 18 weeks were permitted to stand open circuit for the duration of the test. Three of the cells dropped to zero volts and the fourth dropped to 2.2 volts. Some of the cells bulged slightly, indicating that a pressure-producing reaction had occurred. Analysis of gaseous components of the cell indicated the presence of methane. Post mortem of these cells showed that the lithium had been completely consumed; the reddish color of the residue was consistent with products from a lithium-acetonitrile reaction.

These results may indicate that, at the end of the discharge, the lithium underwent a corrosion reaction with the remaining SO₂. It is probable that the corrosion reaction did not begin at the end of discharge, but rather occurred at some rate during the entire discharge period. When the SO₂ was depleted, the lithium was consumed by reaction with acetonitrile, forming the reddish residue and the methane gas (1).

The lithium corrosion probably resulted from the fact that the lithium layer that exists under discharge conditions is not as passivating as that under open circuit conditions. In fact tests on laboratory cells, described

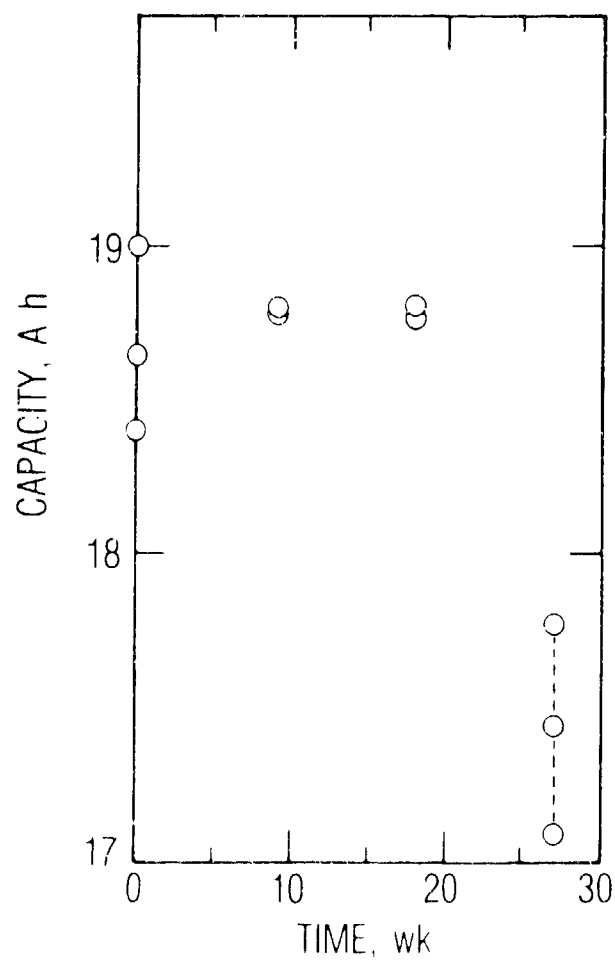


Fig. 2 Time dependence of Li/SO₂ capacity delivered at 70 °F under continuous 500 microamp discharge with weekly pulses (10 minutes at 600 mA).

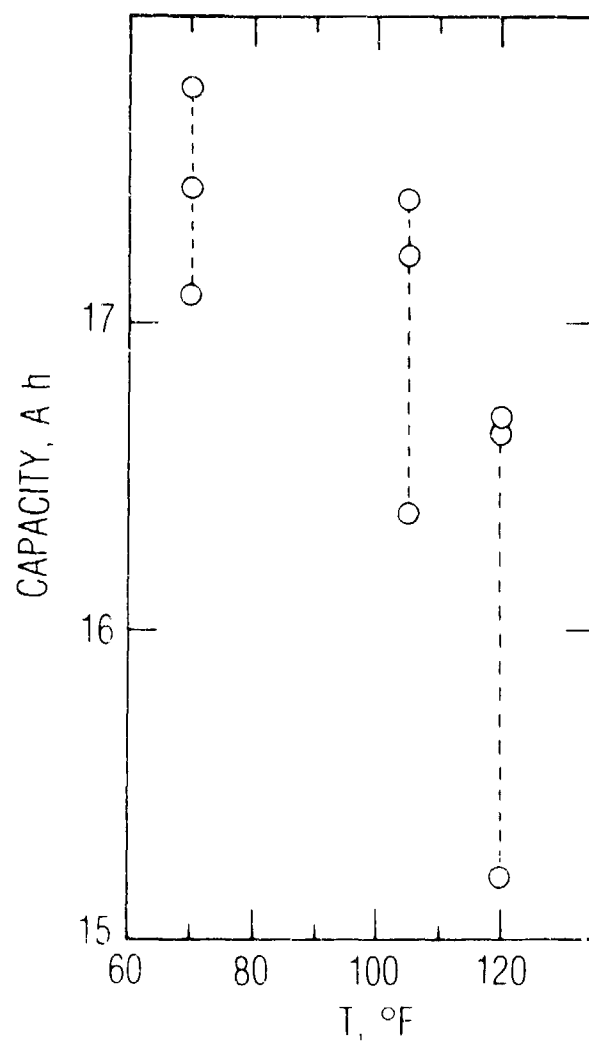


Fig. 3 Temperature dependence of Li/SO₂ capacity delivered after 26 weeks of continuous 500 microamp discharge with weekly pulses (10 minutes at 600 mA).

below, indicated that electrodes partially discharged at high rates suffered a corrosion rate on open circuit about three times higher than electrodes that had never been discharged.

3. Chemistry of the Lithium Passivation Layer

As part of an effort to understand the effects of partial discharge, lithium surface layers from commercial cells that were partially discharged and from cells that were not discharged were analyzed by FTIR, XPS, and IMMA.

The IMMA results are given in Figure 4. Results indicate that the film constituents are Li, S, O, and Br. The Br probably results from precipitated electrolyte, LiBr, on the film. Therefore the primary constituents of the Li surface film are Li-S-O compounds. Figure 4 clearly indicates that the Li layer from the partially discharged cell is thicker than that from the undischarged cell.

The FTIR results are given in Figure 5. The lack of absorption for the Li passivation layer from the undischarged cell is consistent with a thin passivation layer. Assigning the peaks in the FTIR spectra of the partially discharged cell to specific Li-S-O compounds is difficult because reference spectra for these materials are generally not available. However, by using Na analogs for the Li-S-O compounds and assignments made by other workers (6, 13, 14, 15, 16), reasonable assignments can be made. Results for the film on the partially discharged cell are consistent with the Li passivation layer containing $\text{Li}_2\text{S}_2\text{O}_4$ (905, 1020, 1070 cm^{-1}), $\text{Li}_2\text{S}_2\text{O}_5$ (970, 1170 cm^{-1}), and $\text{Li}_2\text{S}_n\text{O}_6$, where $n > 2$ (1200-1250, 1000-1050 cm^{-1}).

The XPS results are consistent with the FTIR assignments. The Li film in the partially discharged cell showed peaks at 163.6 eV, consistent with neutral sulfur, and at 169.0 eV, consistent with sulfur V; $\text{Li}_2\text{S}_n\text{O}_6$ has both neutral sulfur and sulfur V. The Li passivation film in the undischarged cell showed a large peak at 165.8 eV, consistent with sulfur III; $\text{Li}_2\text{S}_2\text{O}_4$ has only sulfur III. Both spectra showed other smaller peaks, indicating that both films contained a mixture of Li-S-O compounds.

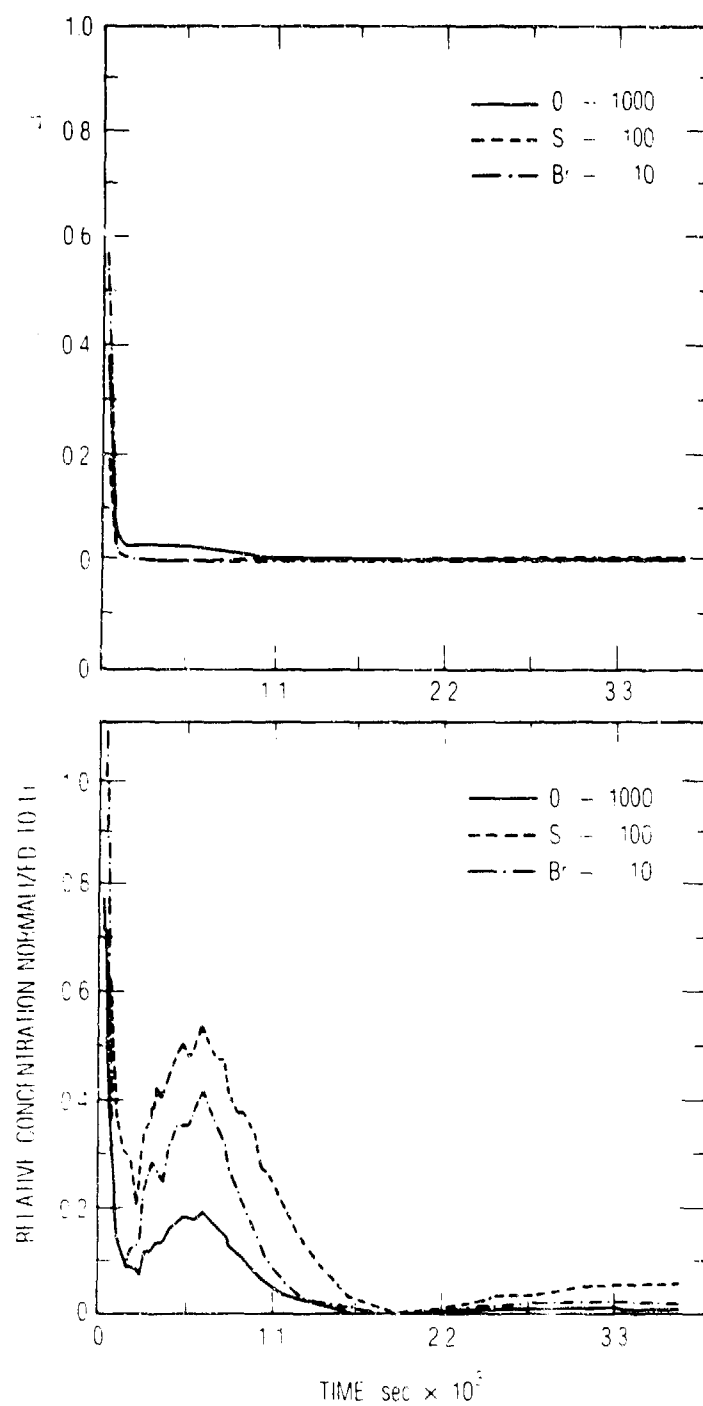


Fig. 4 IMMA results for (A) undischarged and (B) partially discharged Li electrodes from Li/SO_2 cells. The concentration profiles for O, S, and Br are plotted relative to Li. The passivation layer on the partially discharged electrode is thicker than that on the undischarged electrode.

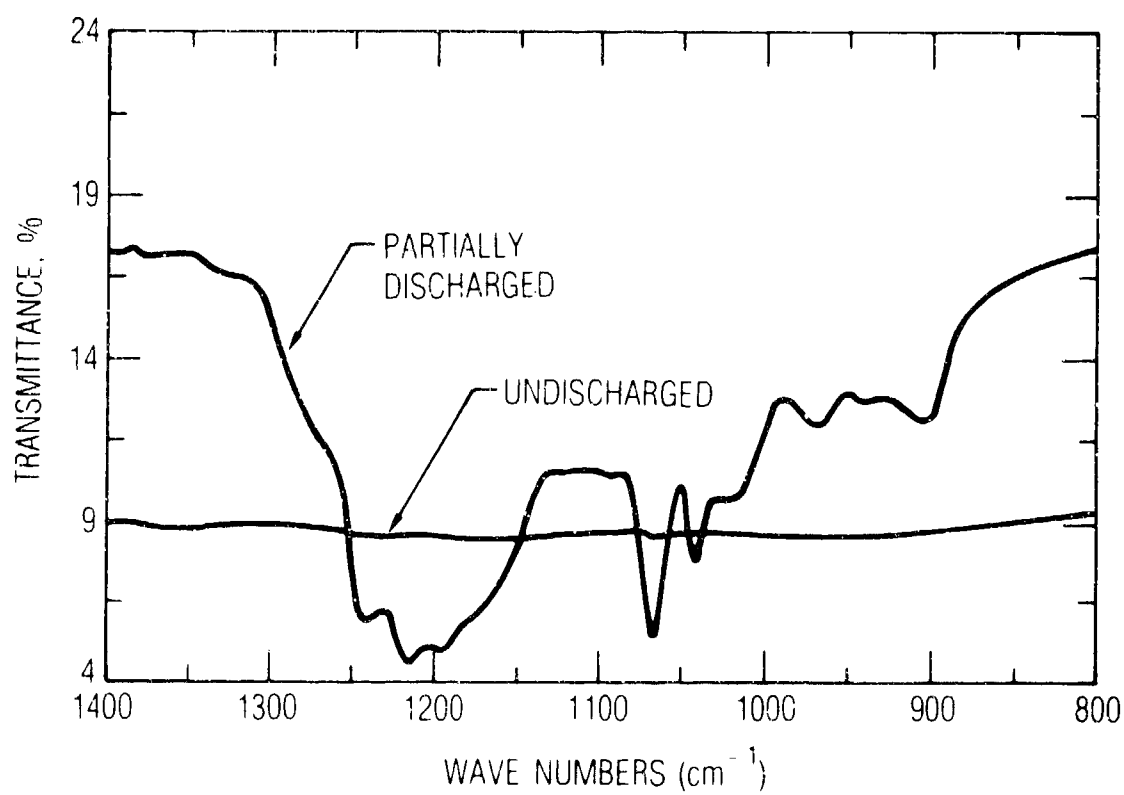


Fig. 5 FTIR spectra of the Li passivation layer for undischarged and partially-discharged Li electrodes from Li/SO₂ cells.

4. Kinetics of Passivation Layer Growth

The growth of the passivation layer was determined by measuring the open circuit impedance of laboratory cells over a period of time beginning immediately after filling the cells with electrolyte. The complex impedance plots are given in Figure 6. By assuming that the lithium/electrolyte interface acts as a parallel plate capacitor, the passivation layer thickness can be calculated by assuming a dielectric constant of 10 (7, 17). Results are given in Figure 7. The growth rate is parabolic, consistent with predicted behavior according to Eq. [1]. The two parabolic regions may correspond to an initial fast film formation followed by slow thickening of the passivation layer.

The specific conductivity of the passivation layer can be obtained from the slope of the curve in Figure 8 (18); the fast-growth region has a specific conductivity of $10^{-9}(\text{ohm-cm})^{-1}$ and the slower growth region $10^{-10}(\text{ohm-cm})^{-1}$. The former value, which corresponds to short time periods, is in good agreement with the value of $4 \times 10^{-9} (\text{ohm-cm})^{-1}$ obtained by Gerenov et al. at comparable times (7).

The constant K in Eq. [1] can now be solved from the slope of the curve in Figure 7 and the specific conductivity derived from Figure 8. The value for K in the slow-growth region is $0.979 \text{ cm}^3/\text{g-cm}^2$. If all of the Li corrosion products precipitate on the lithium surface, then K is essentially a density factor, in units of the reciprocal of the density per area; the calculated density is then 0.85 g/cm^3 . Although no density information is available for the Li-S-O compounds found in the passivation layer by the IR techniques described above, the density of Li_2SO_4 is 2.2 g/cm^3 (19). The low calculated density implies that not all of the Li corrosion products precipitate to form the primary passivation layer.

In analogy with the model put forth by Peled (9) for the Li/SOCl_2 couple, the layer on the Li surface can be interpreted in terms of a thin primary layer, which is responsible for the passivation, and a thicker, porous secondary layer. Accordingly, the Li corrosion products that do not precipitate to form the primary passivating layer precipitate away from the Li surface to form the porous secondary layer.

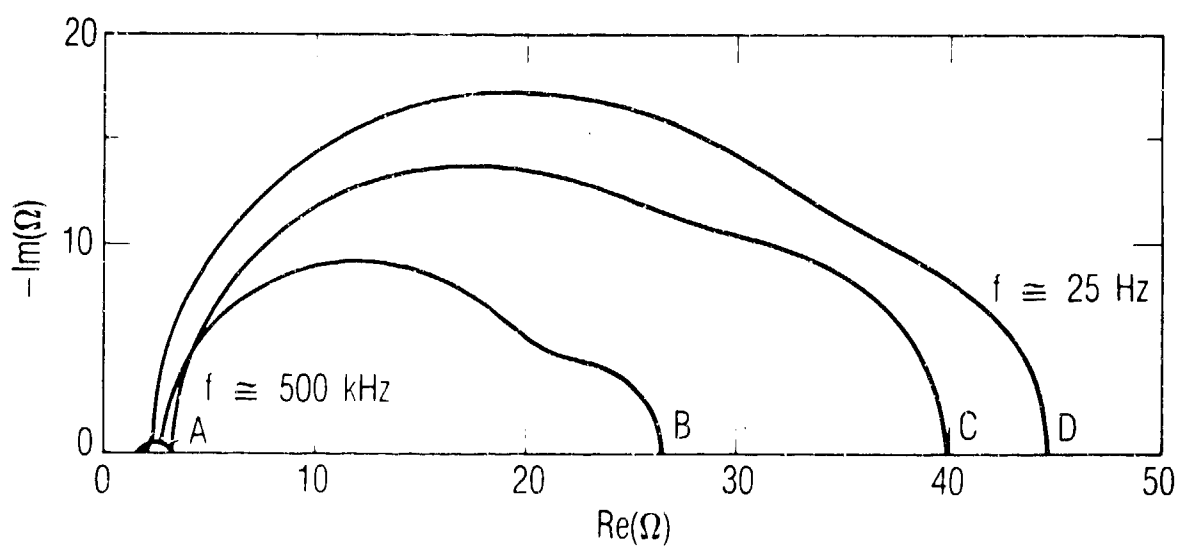


Fig. 6 Impedance of Li electrode stored open circuit in SO_2 electrolyte. Frequency range is 25 Hz - 500 kHz. A: Immediately after electrolyte fill; B: 4 hours, C: 22 hours; D: 364 hours.

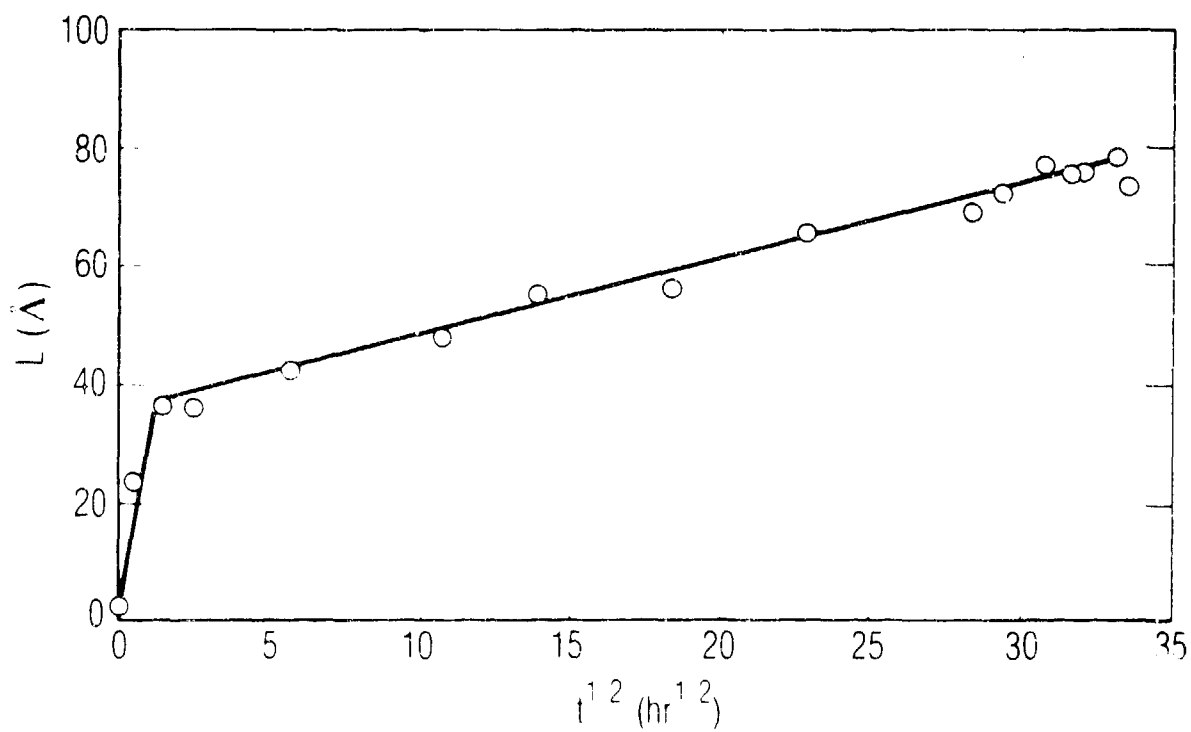


Fig. 7 Primary Li layer thickness as function of $t^{1/2}$; thickness was calculated from impedance results and parallel plate capacitor model.

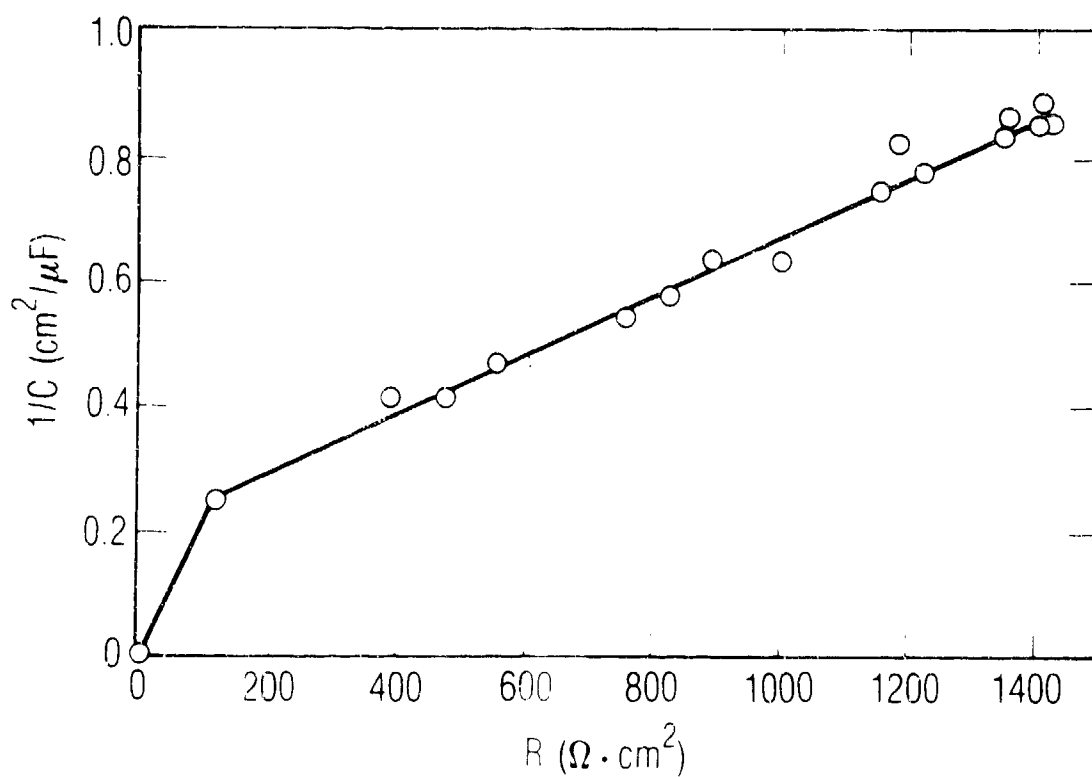


Fig. 8 Reciprocal of capacitance versus resistance for primary layer on undischarged Li electrode in SO_2 electrolyte. Capacitance and resistance values were determined from impedance results.

The effects of partial discharge on the primary passivation layer apparently exacerbate formation of the secondary layer. The effects of discharge on the primary layer are given in Figure 9; the primary layer thickness, as determined by the impedance technique, is given as a function of $t^{1/2}$. A single discharge (12.5 mA/cm^2 for 5 minutes) was applied at $t^{1/2} = 28 \text{ hr}^{1/2}$. On the right hand ordinate, the integrated lithium corrosion current is given, calculated by using the measured electrode impedance as a function of time and a potential drop across the layer calculated from the Nernst equation. The lithium corrosion rate is three times greater after the partial discharge. Despite the higher corrosion rate, the primary layer does not recover to the same thickness. This finding, along with the chemical analysis that indicated thicker layers on partially discharged Li electrodes, is consistent with the excess Li corrosion current leading to precipitation of the secondary layer.

The higher corrosion current after partial discharge may be associated with formation of defects in the primary layer due to the discharge. The defects may be grain boundaries, lattice defects, or cathodic impurities, which result in overall increased electronic conductivity of the primary passivation layer.

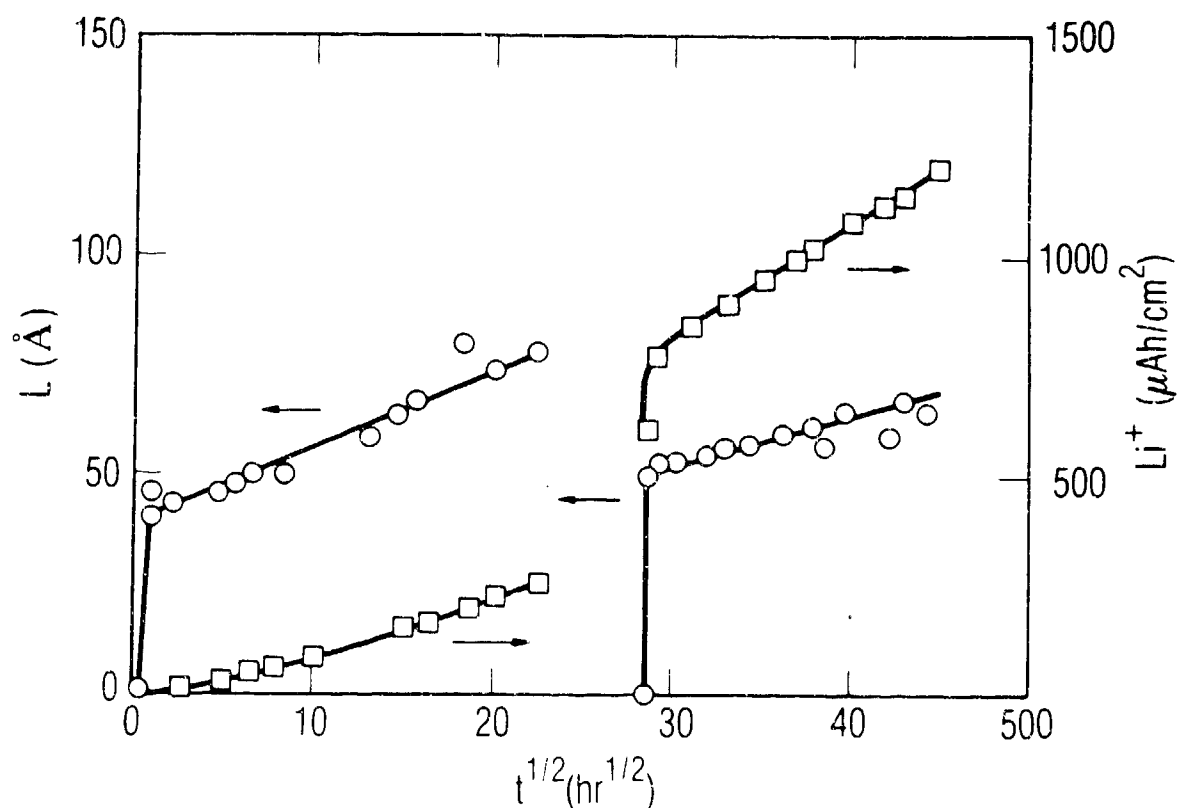


Fig. 9 Effect of partial discharge on Li primary layer and Li corrosion. The left-hand ordinate indicates the primary Li passivation layer thickness as a function of $t^{1/2}$. The right-hand ordinate indicates the integrated Li ion corrosion current as a function of $t^{1/2}$. Li ion corrosion current was estimated by calculating the corrosion current from the measured electrode impedance and by estimating the potential drop across the passivation layer by using the Nernst equation. At $t^{1/2} = 28$ hr^{1/2}, the electrode was given a 5-minute 12.5 mA/cm² discharge. The Li corrosion rate increased by about a factor of 3 after the partial discharge.

V. CONCLUSIONS

The role of lithium passivation in Li/SO_2 cell performance has been studied. Long-term, low rate discharge of commercial cells was observed to degrade capacity; the degradation was attributed to modification of the lithium passivation layer that led to increased lithium corrosion. The degradation was greater at higher temperature. Short-term partial discharge of lithium electrodes was also observed to lead to increased corrosion of the lithium electrode. The corrosion products formed a thick secondary passivation layer. Once formed, the secondary passivation layer induced a secondary polarization on high rate discharge. These results indicate that partial discharge, including periodic testing, of Li/SO_2 cells should be limited in order to preserve high-rate performance.

REFERENCES

1. P. Bro and S. C. Levy, "Lithium Sulfur Dioxide Batteries," in Lithium Battery Technology, H. V. Venkatesetty, editor, The Electrochemical Soc., Inc., Pennington, N. J., 1984.
2. "Lithium/Sulfur Dioxide Primary Battery System," Duracell USA, Bethel, CT, 1982.
3. S. C. Levy, "Long-Term Lithium Battery Tests--II," SAND79-1383, Sandia National Laboratories, Albuquerque, NM, 1980.
4. D. Linden and B. McDonald, J. Power Sources 5, 35 (1980).
5. W. P. Kilroy and C. R. Anderson, J. Power Sources 9, 397 (1983).
6. K. M. Abraham and S. M. Chaudhri, J. Electrochem. Soc. 133, 1307 (1986).
7. Y. Gerenov, B. Puresheva, and R. V. Moshtev, J. Power Sources 9, 273 (1983).
8. Y. Gerenov, B. Puresheva, and B. Pavlova-Stoynov, "AC Impedance Study of Lithium in Sulphur Dioxide Electrolytes," Proceedings of the Third International Meeting on Lithium Batteries, The Electrochemical Society of Japan, 1986, p. 142.
9. E. Peled, "Lithium Stability and Film Formation in Organic and Inorganic Electrolyte for Lithium Battery Systems," in Lithium Batteries, J. P. Gabano, editor, Academic Press, New York, 1983.
10. H. F. Bittner and M. V. Quinzio, "Secondary Lithium Passivation in the Li/SO₂ Couple," Extended Abstracts of the Electrochemical Society Meeting, Vol. 86-1, The Electrochem. Soc. Inc., May 1986, p. 808.
11. H. F. Bittner and M. V. Quinzio, "Secondary Lithium Passivation in the Li/SO₂ Couple," Proceedings of the 3rd International Meeting on Lithium Batteries, The Electrochemical Society of Japan, May 1986, p. 121.
12. H. F. Bittner, C. C. Badcock, M. V. Quinzio, and L. O. Mertz, "The Effect of Low Drain Rates on Li/SO₂ Cell Performance," Proceedings of the 18th Intersociety Energy Conversion Engineering Conference, Society of Automotive Engineers, 1983, p.1483.
13. K. M. Abraham and L. Pitts, J. Electrochem. Soc. 130, 1618, 1983.
14. R. L. Ake, D. M. Oglesby, and W. P. Kilroy, J. Electrochem. Soc. 131, 968. (1984).

15. W. L. Bowden, L. Chow, D. L. Demuth, and R. W. Holmes, J. Electrochem. Soc. 131, 229 (1984).
16. M. W. Rupich, L. Pitts, and K. M. Abraham, J. Electrochem. Soc. 129, 1857 (1982).
17. F. M. Delnick and W. R. Cieslak, "Anodic Behavior of Selected Metals in Neutral $\text{LiAlCl}_4/\text{SOCl}_2$ Electrolyte: Pt, Mo, W, V, Cr, Co, Ni and 316L Stainless Steel," Extended Abstracts of the Electrochemical Society Meeting, Vol. 84-2, The Electrochemical Society, Inc., October 1984, p. 220.
18. R. V. Moshtev, Y. Gerenov, and B. Puresheva, J. Electrochem. Soc. 128, 1851 (1981).
19. Chemistry and Physics Handbook, R. C. Weast, ed., 52nd Edition, The Chemical Rubber Co., Cleveland, Ohio, 1972.

LABORATORY OPERATIONS

The Aerospace Corporation functions as an "architect-engineer" for national security projects, specializing in advanced military space systems. Providing research support, the corporation's Laboratory Operations conducts experimental and theoretical investigations that focus on the application of scientific and technical advances to such systems. Vital to the success of these investigations is the technical staff's wide-ranging expertise and its ability to stay current with new developments. This expertise is enhanced by a research program aimed at dealing with the many problems associated with rapidly evolving space systems. Contributing their capabilities to the research effort are these individual laboratories:

Aerophysics Laboratory: Launch vehicle and reentry fluid mechanics, heat transfer and flight dynamics; chemical and electric propulsion, propellant chemistry, chemical dynamics, environmental chemistry, trace detection; space craft structural mechanics, contamination, thermal and structural control; high temperature thermomechanics, gas kinetics and radiation; cw and pulsed chemical and excimer laser development including chemical kinetics, spectroscopy, optical resonators, beam control, atmospheric propagation, laser effects and countermeasures.

Chemistry and Physics Laboratory: Atmospheric chemical reactions, atmospheric optics, light scattering, state-specific chemical reactions and radiative signatures of missile plumes, sensor out-of-field-of-view rejection, applied laser spectroscopy, laser chemistry, laser optoelectronics, solar cell physics, battery electrochemistry, space vacuum and radiation effects on materials, lubrication and surface phenomena, thermionic emission, photo-sensitive materials and detectors, atomic frequency standards, and environmental chemistry.

Computer Science Laboratory: Program verification, program translation, performance-sensitive system design, distributed architectures for spaceborne computers, fault-tolerant computer systems, artificial intelligence, micro-electronics applications, communication protocols, and computer security.

Electronics Research Laboratory: Microelectronics, solid-state device physics, compound semiconductors, radiation hardening; electro-optics, quantum electronics, solid-state lasers, optical propagation and communications; microwave semiconductor devices, microwave/millimeter wave measurements, diagnostics and radiometry, microwave/millimeter wave thermionic devices; atomic time and frequency standards; antennas, rf systems, electromagnetic propagation phenomena, space communication systems.

Materials Sciences Laboratory: Development of new materials: metals, alloys, ceramics, polymers and their composites, and new forms of carbon; non-destructive evaluation, component failure analysis and reliability; fracture mechanics and stress corrosion; analysis and evaluation of materials at cryogenic and elevated temperatures as well as in space and enemy-induced environments.

Space Sciences Laboratory: Magnetospheric, auroral and cosmic ray physics, wave-particle interactions, magnetospheric plasma waves; atmospheric and ionospheric physics, density and composition of the upper atmosphere, remote sensing using atmospheric radiation; solar physics, infrared astronomy, infrared signature analysis; effects of solar activity, magnetic storms and nuclear explosions on the earth's atmosphere, ionosphere and magnetosphere; effects of electromagnetic and particulate radiations on space systems; space instrumentation.